

Dielectric, Mechanical and Structural, and Water Absorption Properties of a Thermoplastic-Modified Epoxy Resin: Poly(ether sulfone)–Amine Cured Epoxy Resin

Richard A. Pethrick,* Elisabeth A. Hollins, Iain McEwan,
Alexander J. MacKinnon, David Hayward, and Lynda A. Cannon

Department of Pure and Applied Chemistry, Thomas Graham Building, University of Strathclyde, 295 Cathedral Street, Glasgow G1 1XL, U.K.

Stephen D. Jenkins and Patrick T. McGrail

ICI Wilton Materials Research Centre, Wilton, Middlesbrough, Cleveland TS6 8JE, U.K.

Received December 15, 1995; Revised Manuscript Received April 8, 1996^o

ABSTRACT: Dynamic mechanical thermal analysis (DMTA) on a series of poly(ethersulfone)–amine-cured epoxy resin systems indicates phase separation is occurring, in agreement with previous electron microscopic and dielectric observations. Atomic force microscopy (AFM) measurements reveal that the surface roughness changes with composition and is greatest for the cocontinuous phase structure. Dielectric and gravimetric studies are reported on the absorption of water by these resin systems. Gravimetric measurements yield diffusion coefficients, obtained from the initial slopes, which vary slightly with thermoplastic composition. The equilibrium water uptake decreases with increasing thermoplastic content and when normalized by the volume fraction of epoxy resin exhibits a fairly constant value which infers that the majority of the water is dispersed in the epoxy phase. Analysis of the dielectric data at 10 Hz indicates that behavior similar to that obtained from gravimetric analysis is observed outside the cocontinuous phase region. At the cocontinuous composition, anomalous behavior was observed and is attributed to polarization phenomena associated with the microporous structure of the surface of these polymers. Dielectric analysis indicates that the relative rates of absorption depend on the frequency of observation and that there are two extreme types of environment present in these systems. Some of the water molecules are “bound” to hydroxyl groups generated in the cure process and others exist as “free” molecules in microcavities.

Introduction

Incorporation of thermoplastic polymers into a thermoset resin system leads to significant improvements in the mechanical properties of the resultant material.^{1–5} Interest in these materials stems from greater impact strength compared with the unmodified thermoset resin systems and their potential application in the aerospace industry. Ease of processing at low temperatures, high tack, and drape, allowing complex shapes to be fabricated, make these materials very attractive. Liquid carboxy-terminated butadiene–acrylonitrile copolymers (CTBN) have been incorporated into epoxy resins to generate rubber-toughened materials. During the cure process, the CTBN rubber phase separates into micro-sized domains; unfortunately, the rubber particles induce a reduction of the T_g and modulus. The performance of these modified resins in hot/wet conditions is also found to be inferior to that of the unmodified thermosets. Linear high molecular weight thermoplastics are inherently tough and may be expected to reduce the brittleness of a thermoset without affecting their advantageous ultimate properties. Bucknall and Partridge have used ICI's poly(ether sulfone) (PES) in epoxy resin to generate a high-temperature thermoplastic-modified thermoset. Subsequently, different thermoplastics have been studied in epoxy resins by Bucknall, McGrath, and co-workers^{1–4} and Sefton and co-workers.⁵ Thermoplastics have also been studied in other types of thermoset networks.^{6–8}

The poly(ether sulfone)–epoxy resin system has the attraction of forming homogeneous mixtures in the

uncured state; however, on curing, phase separation occurs and differences in physical properties are then observed between mixtures with relatively similar molecular properties. For low thermoplastic contents, spherical domain structures are observed with dimensions which depend on the molecular weight and functionality of the linear polymer. Between 20 and 30% (w/w) thermoplastic a cocontinuous phase is formed and above 30% (w/w) a phase-inverted morphology is generated. The cure characteristics and physical property variations with composition of thermoplastic have been reported previously.^{6–8}

This paper describes the effects of the morphology on the dynamic mechanical and water absorption properties in a poly(ethersulfone)–epoxy resin system.

Experimental Section

Materials. The system investigated was based on the cure of triglycidylaminophenol (Ciba Geigy MY0510) with 4,4'-diaminodiphenyl sulfone (Ciba Geigy HT976) with incorporation of the thermoplastic, Victrex 5003P, poly(ether sulfone) (ICI plc.), having a number-average molecular weight M_n = 24 000. The epoxy resin and hardener were used as supplied in stoichiometric ratio of 1:1 (w/w) and the thermoplastic was dried before use. Samples were produced by dissolving the thermoplastic in methylene chloride. The epoxy and hardener were then added before the solvent was mostly boiled off, leaving an apparently homogeneous solution. The blend was then poured into an open mold (dimensions 14 cm × 10 cm), which had been preheated to 140 °C, and degassed for 30 min under vacuum to remove residual solvent and trapped air. The samples were then cured at 180 °C for a further 120 min and allowed to cool to room temperature over a further 120 min. The films had a thickness of ~0.1 cm and were used for all the physical measurements described in this study. A range

* To whom correspondence should be addressed.

^o Abstract published in *Advance ACS Abstracts*, June 1, 1996.

of samples with varying thermoplastic content (0–30% (w/w)) was made in each case.

Dynamic Mechanical Analysis. A Polymer Laboratories dynamic mechanical thermal analyzer (DMTA) was used at a frequency of 1 Hz and a strain of $\times 4$, and the temperature was scanned at 3° min^{-1} from a starting temperature of 30°C up to just above the glass transition temperature (T_g). The samples for test were prepared with dimensions of $20 \text{ mm} \times 10 \text{ mm}$ and a thickness of $0.8\text{--}1.6 \text{ mm}$ and were subjected to forced oscillation using a single cantilever mode of action.

Gravimetric Measurements. Cast films were used to measure water uptake by weight gain as a function of time. Samples were immersed in deionized water at 25°C and weighed periodically using a Mettler M5 balance. The samples were removed from the water and wiped to remove excess water, after 4 min the samples were weighed and reimmersed after 5 min total out of water.

Low-Frequency Dielectric Measurements. The resin sheets were covered by a 1000 \AA layer of silver, which was deposited by evaporation, and the resultant sandwich structure forms a capacitor. The films were then encased in a silicon sealant with only one face of the film exposed. The metal layer on this face is sufficiently thin to allow rapid moisture transfer but also sufficiently coherent so as to achieve a low electrical resistance required for used as an electrode. The samples were then immersed in deionized water at 25°C and the dielectric response measured at set intervals over the frequency range of $10^{-2}\text{--}10^5 \text{ Hz}$ using a dielectric spectrometer.⁹ After the first 18 h of measurement, the change in dielectric response was slow enough to be measured to 10^{-3} Hz .

Atomic Force Microscopy. Micrographs of small sections of the resin sheets were recorded with a Burleigh ARIS-3300 Personal AFM. A standard Burleigh AFM probe was used for the measurements. The cantilever shape was rectangular with a length of $10\text{--}15 \text{ }\mu\text{m}$ and a silicon pyramidal tip with a spring constant of $\sim 0.05 \text{ N m}^{-1}$. Surfaces were imaged at a constant force. The sample was moved in the $x\text{--}y$ plane and a voltage was applied which moved the piezo driver over the z axis in order to keep the probing force constant, resulting in a 3D height image of the examined surface. The force applied to the surface was typically 5 nN .

Results and Discussion

Dynamic Mechanical Analysis. Analysis of the thermoset system with no thermoplastic (Figure 1) indicates the presence of a glass transition process (T_g) at 265°C and an initial softening point at $\sim 230^\circ \text{C}$. In the modified systems an initial softening point at $\sim 200^\circ \text{C}$ due to the thermoplastic incorporation is observed and corresponds to the T_g of the thermoplastic phase. The fact that two well-separated processes are observed is consistent with electron microscopy observations of a two-phase structure in these systems^{5,6,10–11} and indicates that only limited intermixing of the two phases occurs. The temperature at which these two processes occurs is changing with composition of the thermoplastic, and the amplitude of the loss peak increases with increasing thermoplastic content. The fact that the amplitude increases proportional to volume fraction of thermoplastic is consistent with the concept of extensive phase separation in these systems. The temperature at which the loss process occurs does start to change at high thermoplastic content, indicating that some mixing of the two phases is taking place, and possibly reflects curing of dissolved epoxy on the thermoplastic relaxation.

Previous differential scanning calorimetry measurements have been carried out on these systems by

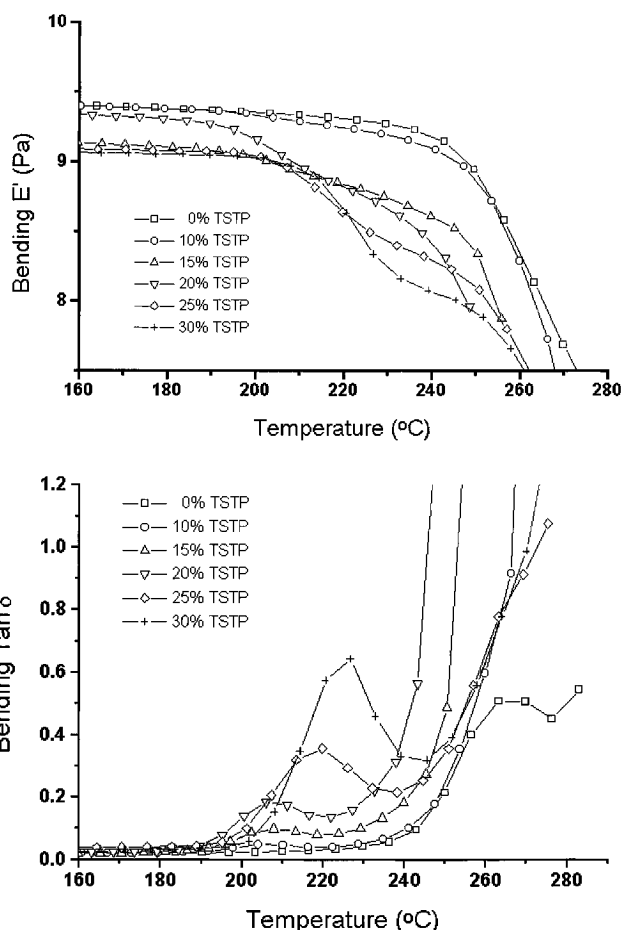


Figure 1. DMTA traces for thermoset/thermoplastic: (a) tensile modulus; (b) loss modulus.

Table 1. DSC Glass Transition Temperature Calculated by MacKinnon et al.

thermoplastic content (%)	DSC T_g ($^\circ \text{C}$)	DMTA T_g ($^\circ \text{C}$)
0.0	222.1	265.8
5.4	212.7	
11.0	219.4	206.5
15.6	190.9	207.8
20.6	196.1	207.5
26.7	203.1	218.6
30.0	223.6	224.8

MacKinnon et al.⁷ Those measurements showed that the T_g of the cured unmodified resin differed significantly from those of the epoxy/thermoplastic blends with a progressive decrease in the value of T_g with increasing thermoplastic content up to $\sim 20 \text{ wt } \%$. Above $20 \text{ wt } \%$ the value of the T_g became almost constant, indicating no further effect of addition of thermoplastic. The DSC values calculated by MacKinnon et al.⁷ are presented in Table 1. The DSC results lie between the values of the T_g 's observed by dynamic mechanical measurements and indicate that the DSC data is unable to resolve the two T_g processes satisfactorily and is measuring some averaged value. The values of the T_g 's obtained by DMTA are presented in Table 1.

Electron micrographs for this and related systems have been reported previously^{5,6,10,11} and indicate changes in the phase structure with composition. In the present systems between 0 and $2.5 \text{ wt } \%$ thermoplastic, a homogeneous solution is observed. Concentrations in the range $5\text{--}20 \text{ wt } \%$ produce a particle phase which changes into a cocontinuous phase at $25\text{--}30 \text{ wt } \%$.

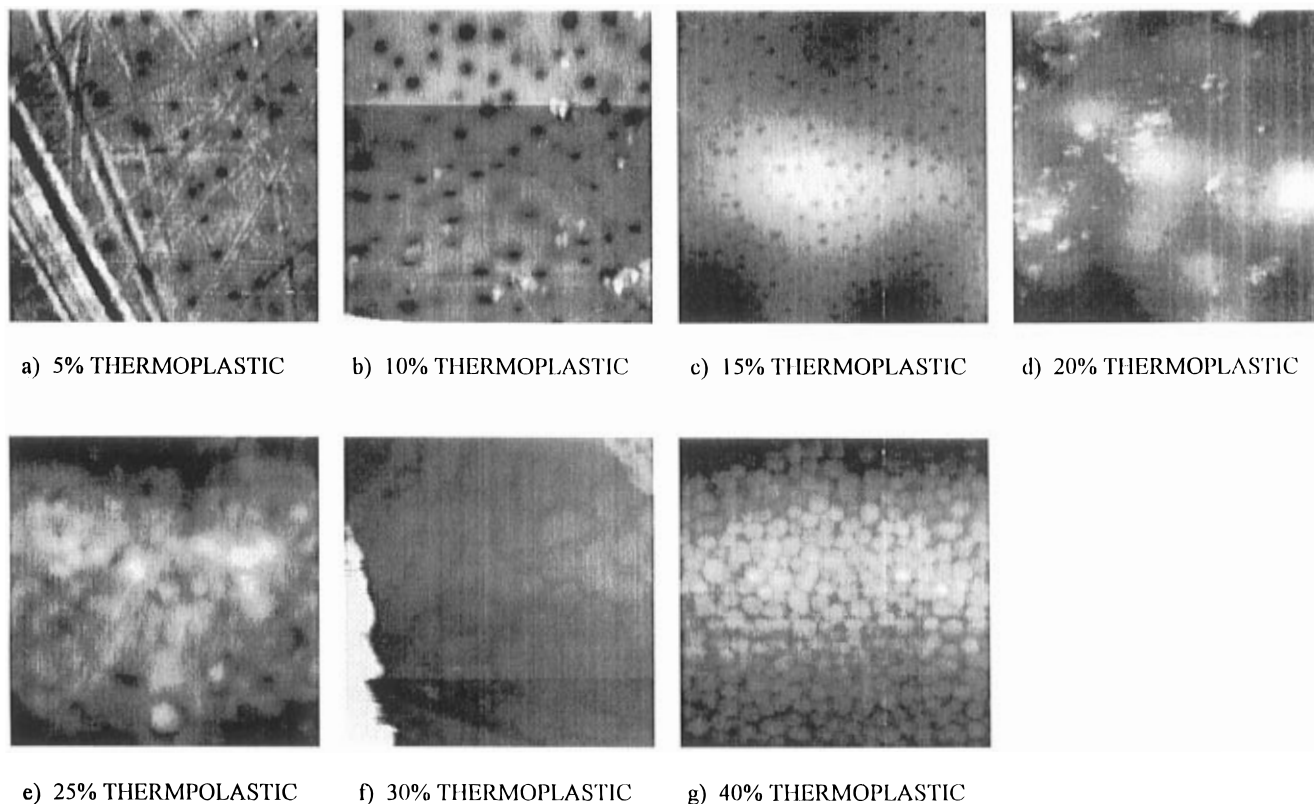


Figure 2. AFM scans for different thermoplastic contents (scan area $5\ \mu\text{m} \times 5\ \mu\text{m}$).

Above 30 wt % phase inversion occurs, the continuous phase now being thermoplastic rich. The DMTA measurements are consistent with these changes with the loss of the modulus occurring at high temperatures once the cocontinuous phase structure has been formed.

Atomic Force Microscopy. Two-dimensional surface images of epoxy with varying amounts of thermoplastic were produced for the samples studied (Figure 2). Changing the composition of the thermoplastic causes a change in the surface texture which parallels closely with that observed with electron microscopy. The AFM study allows not only imaging of the surface but also an estimation of the surface roughness. Although to the eye the samples look smooth, the AFM reveals that changes in the composition produce variations in surface texture. In the low-concentration range, the dispersed phase is the thermoplastic, and differences in surface tension and mechanical forces present during cure lead to very small pores being present when the occluded phase breaks the surface. The sizes of the features observed correspond very closely to those imaged by electron microscopy. Similarly above 25% the surface texture reflects the phase separation of the epoxy phase. At 20% thermoplastic, the system exists as a cocontinuous phase and the surface morphology is much rougher as a consequence of the differences in surface energy and the larger size of the structures involved. The surface indentations for the 20% sample are typically $\sim 50\ \text{nm}$ whereas for the other compositions the indentations are $\sim 10\text{--}20\ \text{nm}$ or less. The maximum change in the surface depth for each of the samples can be seen in Table 2.

Similar measurements have been performed on the same epoxy system with the diglycidyl ether of Bisphenol F (DGEBA) added and using an amine-terminated polysulfone (RT-PS) as the thermoplastic.⁷ The system using RT-PS as the thermoplastic also showed increased roughness around the cocontinuous phase but the phase

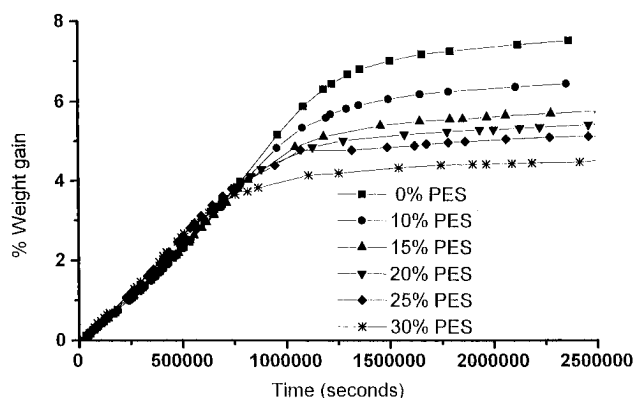


Figure 3. Gravimetric diffusion curves.

Table 2. Maximum Surface Variations from AFM Measurements

thermoplastic content (%)	max diff in depth (nm)
5	20
10	30
15	30
20	70
25	25
30	25
40	15

structure is much smaller for this system and the indentations observed are an order of magnitude smaller in size.

Water Sorption Studies. Gravimetric Measurements. The sorption of water for samples with varying thermoplastic content were investigated (Figure 3). Although the sorption processes of liquids and vapor in glassy polymers follow complex water diffusion mechanisms in epoxy resin matrices, their behavior has frequently been found to approximate to that corre-

sponding to Fickian diffusion.^{12–14} The characteristics of Fickian diffusion have been described by Fujita¹⁵:

(i) The sorption curves are linear in the initial stages.
 (ii) Above the linear portion both absorption and desorption curves are concave to the abscissa. For absorption the linear region extends to over 60% or more of the region studied.

(iii) When a series of reduced absorption curves are plotted for films of different thickness, the curves are superimposable.

If a plane polymer sheet is exposed to a fluid, the change of the concentration (C) of a diffusing substance as a function of time (t) and position (x) is given by Fick's second law.¹⁴

$$\frac{\partial C}{\partial t} = D \frac{\partial^2 C}{\partial x^2} \quad (1)$$

where D is the diffusion coefficient. If the material has a uniform initial diffusant concentration (C_0) and the surface is kept at a constant concentration C_{\max} , the solution of eq 1 is¹³

$$\frac{C - C_0}{C_{\max} - C_0} = 1 - \frac{4}{\pi} \sum_{n=0}^{\infty} \frac{(-1)^n}{2n+1} \exp[-D(2n+1)^2 \pi^2 t / h^2] \cos \frac{(2n+1)\pi x}{h} \quad (2)$$

where n is an integer from 0 to ∞ . The total amount of substance diffusing in the polymeric material (M) as a function of time is given by the integral of eq 2 across the thickness (h):

$$\frac{M}{M_{\max}} = 1 - \frac{8}{\pi^2} \sum_{n=0}^{\infty} \frac{1}{(2n+1)^2} \exp[-D(2n+1)^2 \pi^2 t / h^2] \quad (3)$$

where M_{\max} is the equilibrium value of the diffusing substance at infinite time and is estimated from diffusion plots by an extrapolation technique.¹⁶ The diffusion plots show an initial Fickian type absorption and then a slow linear increase associated with plasticization of the matrix and reflect long-term changes with water uptake. The value of M_{\max} is taken as the extrapolated value of the initial data¹⁶ and does not account for the long-time plasticization effects which will not be described by eq 3. A simplified form of eq 3 for values of M/M_{\max} lower than 0.6¹⁴ has the form

$$\frac{M}{M_{\max}} = \frac{4}{h\sqrt{\pi}} \sqrt{Dt} \quad (4)$$

For gravimetric analysis eq 4 is a valid representation of the time dependence of the water uptake. The calculated diffusion coefficients are presented in Table 3. The results indicate that on increasing the amount of thermoplastic in the system leads to a decrease in the total amount of water adsorbed by reducing the amount of epoxy. The water uptake compared to the percentage of epoxy is reasonably constant (Table 4), which implies that the water is concentrated in the epoxy phase and little is present in the thermoplastic phase.

Table 3. Gravimetric and Dielectric Diffusion Coefficients

resin system	dielectric diffusion coeff ($D \times 10^{10} \text{ cm}^2 \text{ s}^{-1}$)	gravimetric diffusion coeff ($D \times 10^{10} \text{ cm}^2 \text{ s}^{-1}$)
TGAP/DDS + 0% PES	5.09	4.46
TGAP/DDS + 10% PES	13.42	8.18
TGAP/DDS + 15% PES	4.55	5.18
TGAP/DDS + 20% PES	60.5 ^a	5.76
TGAP/DDS + 25% PES	5.42	8.49
TGAP/DDS + 30% PES	6.10	8.37

^a For this measurement the cocontinuous phase structure is probably unreliable because the dielectric measurements will be reflecting the microporosity of this structure and hence do not conform to the simple model presented above.

Table 4. Gravimetric Results

resin system	% water	% water/% epoxy
TGAP/DDS + 0% PES	7.4	0.074
TGAP/DDS + 10% PES	6.3	0.070
TGAP/DDS + 15% PES	5.5	0.065
TGAP/DDS + 20% PES	5.3	0.066
TGAP/DDS + 25% PES	5.0	0.066
TGAP/DDS + 30% PES	4.4	0.063

Dielectric Measurements of Water Absorption.

The dielectric measurements were performed over the frequency range 10^{-3} – 10^5 Hz over a period of 2 weeks at 25 °C. The results for the dielectric permittivity and loss with time and frequency can be seen in Figure 4. The observed shifts or increases in the dielectric loss at low frequencies are associated with a general upward shift in the T_g process on the frequency domain, consistent with plasticization and lowering of the value of T_g . The apparent random increase and then decrease and then subsequent increases and decreases are consistent with the plasticization process leading to local rearrangement of the chain structure in the matrix and relaxation of stresses inducing changes in the local packing. The initially cured matrix will contain stresses left due to the vitrification processes freezing in structure to the system. Plasticization will lead to a lowering of the value of T_g , consistent with a shift to higher frequencies of the dielectric loss. The increase in local mobility will however allow further reaction to be induced in the matrix and this will in turn lead to an increase in the value of T_g and a reduction in the dielectric loss at low frequency. Further ingress of moisture will once more plasticize the system and lead to an increase in the loss. It is clear from the data that the plasticization and advancement of cure are continually shifting the T_g process but the overall effect is one of plasticization as reported by many workers using more conventional measurements of the bulk T_g . It must be remembered that the dielectric data sees the microscopic changes occurring in the system and is revealing subtle changes not necessarily seen by bulk measurements of T_g .

By examining the water uptake plots (Figure 4), values of ϵ'_{∞} were taken at 10^5 Hz for the initial "dry" permittivity reading, which is assumed constant and is used in subsequent calculations, and for the final permittivity reading. The dielectric increment of these values $\Delta\epsilon'_{\infty}$ relates to the amount of "free" water present in the system. At 10 Hz the dielectric increment $\Delta\epsilon'$ relates to the "bound" and "free" water in the system.

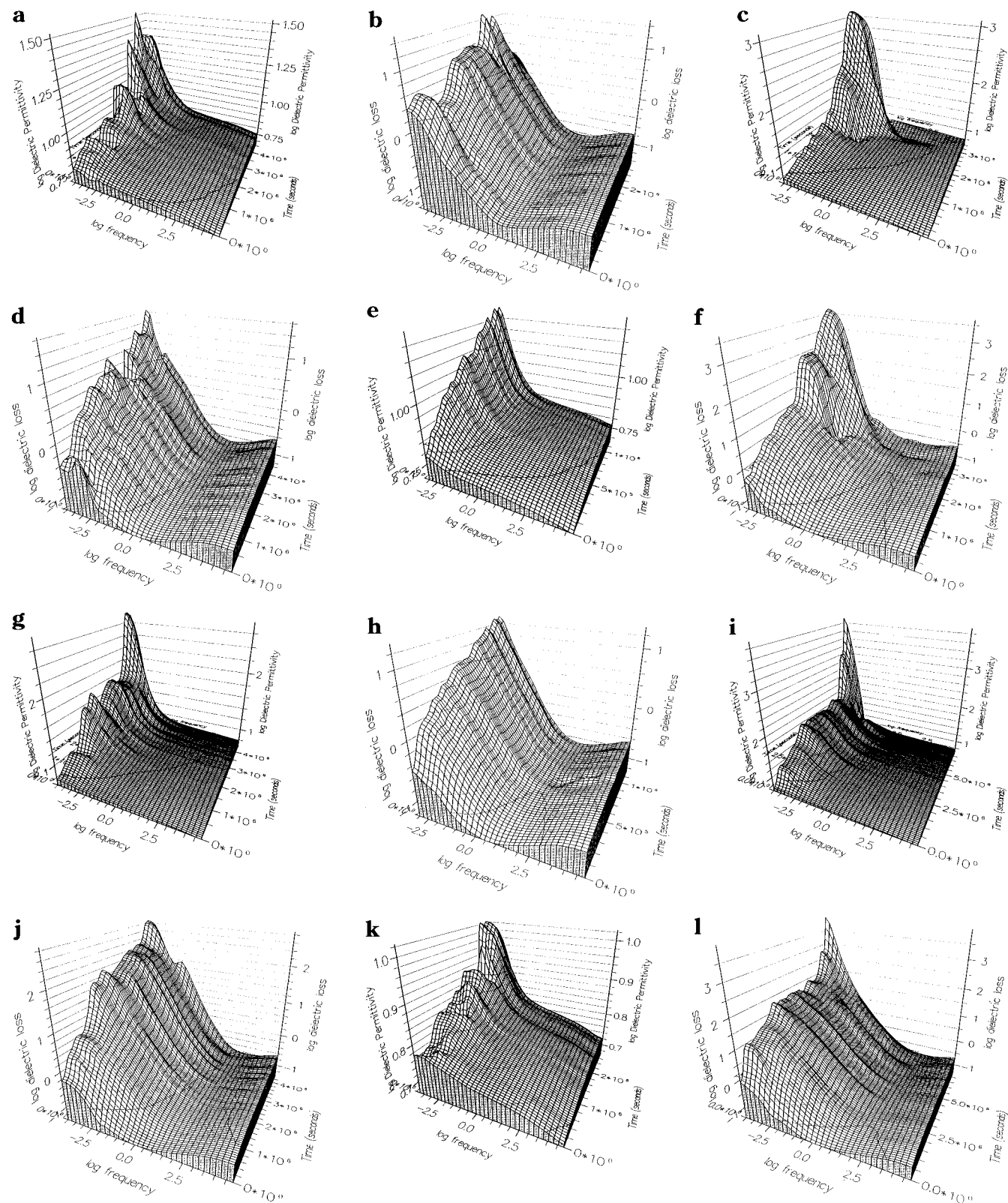


Figure 4. Dielectric permittivity and loss for 0% thermoplastic ((a) permittivity; (b) loss), 10% thermoplastic ((c) permittivity; (d) loss), 15% thermoplastic ((e) permittivity; (f) loss), 20% thermoplastic; ((g) permittivity; (h) loss), 25% thermoplastic ((i) permittivity; (j) loss), and 30% thermoplastic ((k) permittivity; (l) loss).

The difference between the two increment values gives a measure of the amount of water which is intimately bound to the hydroxyl groups generated on curing the system. The water bound to these groups leads to an increase in the dielectric loss in this region without significant shift in the locus of the relaxation process and the calculated values for the "bound" and "free" water were obtained (Table 5). The contribution from

"free" water is associated with dipolar relaxation processes occurring above 10^6 Hz and located around 10^{11} Hz.¹⁰⁻¹¹ In other systems it has been observed that dipolar processes with characteristics similar to those of liquid water can be observed and have been associated with segregation of water into microvoids with dimensions of $\sim 0.01 \mu\text{m}$ or less. The dielectric results show that apart from an initial reduction in the amount

Table 5. Calculated Values of Bound and Free Water

resin system	$\Delta\epsilon'$	$\Delta\epsilon'$ (bound)	$\Delta\epsilon'$ (free)	% bound	% free
TGAP/DDS + 0% PES	1.005	0.297	0.708	29.6	70.4
TGAP/DDS + 10% PES	1.428	0.281	1.147	19.7	80.3
TGAP/DDS + 15% PES	1.934	0.365	1.569	18.9	81.1
TGAP/DDS + 20% PES	1.505	0.286	1.225	18.6	81.4
TGAP/DDS + 25% PES	1.972	0.392	1.580	19.9	80.1
TGAP/DDS + 30% PES	1.942	0.396	1.546	20.4	79.6

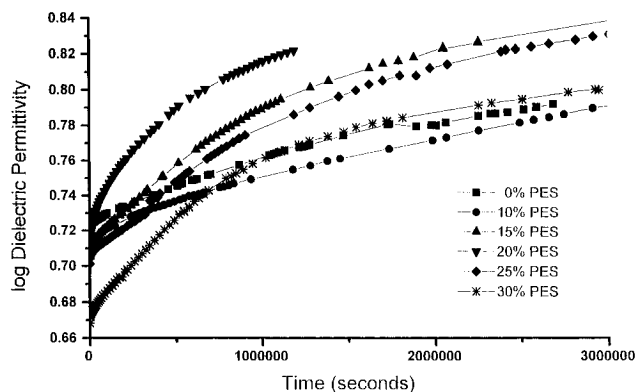
of free water with the addition of thermoplastic, increasing the amount of thermoplastic does not significantly affect the ratio of bound and free water in the systems. This observation is consistent with the assumption that the water is predominantly located in the epoxy phase.

Evolution of the dielectric permittivity with time is directly related to the diffusion of water into the capacitor structure and hence can be used to estimate the diffusion coefficient. Starting from eq 4, it is necessary to derive an equation which describes the situation used in the experiments. The cell used for the dielectric study allows diffusion from one side only, the edges and reverse side being sealed with silicone rubber and a copper electrode, respectively. The theory describing the gravimetric measurements involves the concentration of the water molecules whereas the dielectric experiment measures the change in the permittivity of the media. Under isothermal conditions, the increase in the permittivity observed during water diffusion ($\epsilon' - \epsilon'_0$) is proportional to the number of water dipoles present in the system.¹⁷⁻¹⁸ Therefore, a linear relationship between ϵ' and the water concentration in the polymer is expected. It is assumed that the thickness (h) does not change with water concentration. It has, however, been pointed out previously^{13,17,19} that there is observed a discrepancy between the observed increment and that predicted on the basis of the amount of water absorbed. The permittivity of free water is 80.4 at 293 K and apparent discrepancies between predicted and theory have been reported.¹⁷⁻²⁰ The water molecules may be assumed to be either clustered, in which case the dielectric increment should closely correlate with the value for water, or bound to the matrix, in which case a lower value may be expected. In the case of the dielectric analysis, the diffusion can be modeled according to the following equation:

$$\frac{\epsilon' - \epsilon'_0}{\epsilon'_{\max} - \epsilon'_0} = 1 - \frac{4}{\pi} \sum_{n=0}^{\infty} \frac{(-1)^n}{2n+1} \exp[-D(2n+1)^2 \pi^2 t / h^2] \quad (5)$$

where ϵ'_{\max} is the maximum value of the dielectric permittivity achieved by the water diffusing into the polymer matrix and ϵ'_0 is the value of the dielectric permittivity at time = 0. In this case the diffusion coefficient (D) can be estimated by considering only the first term in eq 5 (i.e., $n = 0$) and by plotting the root of time ($t^{1/2}$) against the normalized dielectric permittivity: $(\epsilon' - \epsilon'_0)/(\epsilon'_{\max} - \epsilon'_0)$, with the condition that $\exp[-D\pi^2 t^{1/2} / h^2] < 1$. Thus

$$D = -\frac{h^2}{t^{1/2} \pi^2} \ln\left[\frac{\pi}{8}\right] \quad (6)$$

**Figure 5.** Dielectric diffusion curves at 10 Hz and 25 °C.

Furthermore, eq 6 can be written in the approximate form

$$D = 0.0947 h^2 / t^{1/2} \quad (7)$$

It has been previously observed that measurements of the diffusion permittivity at different frequencies lead to different values of the apparent diffusion coefficient,¹⁹ lower apparent values being observed at higher frequencies. It is assumed that the variation of the dielectric permittivity measured at 10 Hz (Figure 5) reflects the total relaxation spectrum of the water molecules in the matrix and hence is correlated with the total sorption process. The curves obtained are similar to those observed by gravimetric measurements but the 20% thermoplastic sample shows variations not observed in the gravimetric data.

The dielectric diffusion coefficients were calculated from the dielectric permittivity at 10 Hz. The results can be seen in Figure 5 and the diffusion coefficients are shown in Table 3. The diffusion coefficients which were obtained are similar to those obtained from gravimetric results with the exception of the 20% thermoplastic sample, which had an extremely high diffusion coefficient, with a repetition of the experiment confirming this result. The initial high value of the dielectric permittivity on exposure to water would be consistent with there being a contribution to the polarization due to the presence of a porous structure next to the electrode associated with the cocontinuous structure of the material and phase separation. The dielectric measurement reflects the top 10 nm of the sample next to the electrode, which reaches equilibrium in the first few minutes. These observations are consistent with the increased roughness of these samples in the cocontinuous region. Once diffusion has started, the effects of these surface anomalies are lost and the change in the dielectric profile with time takes on a more normal form. Subsequent changes will be controlled by the same diffusion processes that control the mass variation with time and hence at longer times the dielectric curves assume a more normal form. However, the presence of the microporous surface structure still exhibits itself as a higher value of the permittivity with the data over and above the surface contribution, consistent with data where the surface contribution is not observed.

Previous positron annihilation studies carried out by Mackinnon et al.⁸ have showed that the free volume within the system initially increases and then decreases on addition of thermoplastic and increases again when approaching 30 wt % thermoplastic, indicating that the distribution of free volume in the system is a reflection of the delicate balance of factors which control the final

phase structure. The observed variation in the diffusion coefficients calculated from the initial slope of the normalized weight gain curve parallel the positron results, the diffusion coefficient going through a minimum as the composition is varied.

Conclusions

The above study shows that increasing the amount of thermoplastic in an epoxy system has the effect of reducing the amount of water sorption in the system. DMTA data showed the existence of phase separation within the systems, with the glass transition process being visible for both phases, and that the temperature of these processes is not significantly affected by composition change. Gravimetric results showed that the amount of water adsorbed was reduced as the amount of thermoplastic was increased, which was a reflection that the water is present only in the epoxy phase. The calculated diffusion coefficients were consistent with previous results, with the diffusion coefficient going through a minimum at about 20% thermoplastic, reflecting the delicate balance of factors which control the final phase structure. Analysis of the dielectric results showed that as water was adsorbed, plasticization and advancement of cure are continually shifting the T_g process, but the overall effect is one of plasticization. Dielectric diffusion coefficients were consistent with gravimetric results with the exception of the 20% thermoplastic sample, which indicated the presence of a porous structure next to the electrode. This was confirmed by atomic force microscopy results which showed an uneven morphology of this composition compared to the other compositions.

Acknowledgment. I. McEwan wishes to thank the EPSRC for provision of a postdoctoral assistantship and L. Cannon for an Industrial CASE award sponsored by ICI Paints Division. Support of the Marine Technology

Directorate for D. Hayward, a co-operative award with ICI for A. MacKinnon and an EMR studentship for E. Hollins are gratefully acknowledged.

References and Notes

- (1) Bucknall, C. B.; Partridge, I. K. *Polym. Eng. Sci.* **1986**, *26*, 54.
- (2) Bucknall, C. B.; Partridge, I. K. *Polymer* **1983**, *24*, 639.
- (3) Bucknall, C. B.; and Gilbert, A. H. *Polymer* **1989**, *30*, 213.
- (4) Cecere, J. A.; Senger, J. S.; McGrath, J. M. *32nd Int. SAMPE Symp.* **1987**, p 1276.
- (5) Sefton, M. S.; McGrail, P. T.; Peacock, J. A.; Wilkinson, S. P.; Crick, R. A.; Davies, M.; Almen, G. *19th Int. SAMPE Tech. Conf.* **1987**, p 700.
- (6) MacKinnon, A. J.; Jenkins, S. D. McGrail, P. T.; Pethrick, R. A. *Macromolecules* **1992**, *25*, 3492.
- (7) MacKinnon, A. J.; Jenkins, S. D.; McGrail, P. T.; Pethrick, R. A. *Polymer* **1993**, *34*, 3252.
- (8) MacKinnon, A. J.; Jenkins, S. D.; McGrail, P. T.; Pethrick, R. A. *Polymer* **1994**, *35*, 5319.
- (9) Hayward, D.; Gawayne, M.; Mahboubian-Jones, B.; Pethrick, R. A. *J. Phys. E: Sci. Instrum.* **1984**, *17*, 683.
- (10) Hill, N. E.; Vaughan, W. E.; Price, A. H.; Davis, M. *Dielectric Properties and Molecular Behaviour*; van Nostrand Reinhold Co., New York, 1969.
- (11) Huang, Y.; Kinloch, A. J.; Yuen, M. L. *Third European Symposium on Polymer Blends*; Plastics and Rubber Institute: London, 1990, E5/1.
- (12) Mikols, W. J.; Seferis, J. C.; Apicella, A.; Nicolais, L. *Polym. Compos.* **1982**, *3*, 118.
- (13) Apicella, A.; Egiziano, L.; Nicolais, L.; Tucci, V.; *J. Mater. Sci.* **1988**, *23*, 729.
- (14) Crank, J. J. In *The Mathematics of Diffusion*; Clarendon Press: Oxford, 1975.
- (15) Crank, J. J.; Park, G. S. *Diffusion in Polymers*; Academic Press: London, 1968.
- (16) Johncock, P.; Tudgey, G. F. *Br. Polym. J.* **1986**, *18*, 292.
- (17) Aldrich, P. D.; Thurow, S. K.; McKennon, Lyssy M. E. *Polymer* **1989**, *28*, 2289.
- (18) Pathmanathan, K.; Johari, G. P. *Polymer* **1988**, *29*, 303.
- (19) Maxwell, I. D.; Pethrick, R. A. *J. Appl. Polym. Sci.* **1983**, *28*, 2363.
- (20) Maffezzoli, A. M.; Peterson, L.; Seferis, J. C.; Kenney, J.; Nicolais, L. *Polym. Eng. Sci.* **1993**, *33*, (2), 75–82.

MA9518464